Supplementary Information

Regulation of activity interface in Ni-Co-Mn ternary aerogel catalysts for efficient Water Splitting

Lei Ma[1], Zhi Chen[1]*, Yongkang An[1], Chengzhi Pang[1], Fei Liang[2], Shiwen Wang[1], Xusheng Wang[1], Shengbin Wang[1], Sizhe Wang[2,3]*

[1] Research and Development Department(R&D), Shijiazhuang Shangtai Technology Co., Ltd. Shijiazhuang, Hebei Province 052463, China

[2] Yangtze Delta Region Institute (QuZhou), University of Electronic Science and Technology of China, 324000, China

[3] School of Materials Science and Engineering Shaanxi Key Laboratory of Green Preparation and Functionalization for Inorganic Materials Shaanxi University of Science & Technology

* Corresponding author: drzhichen@163.com; kevinwang@sust.edu.cn

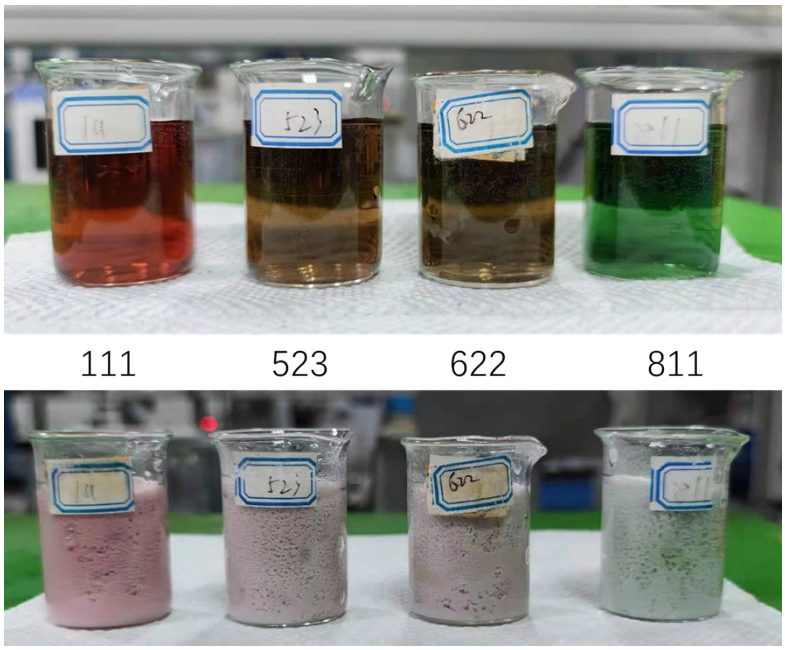

Figure S1. Optical photographs of the precursor solution and the resulting wet gel.

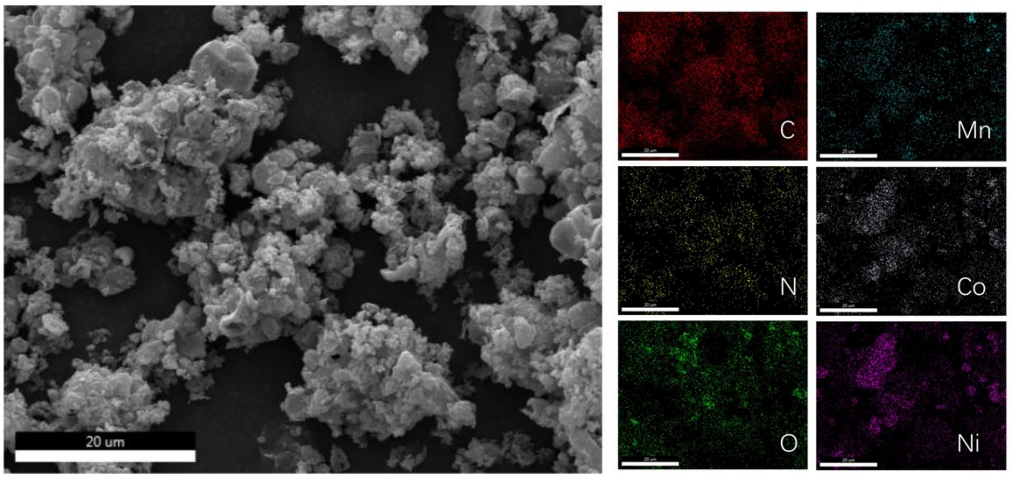

a

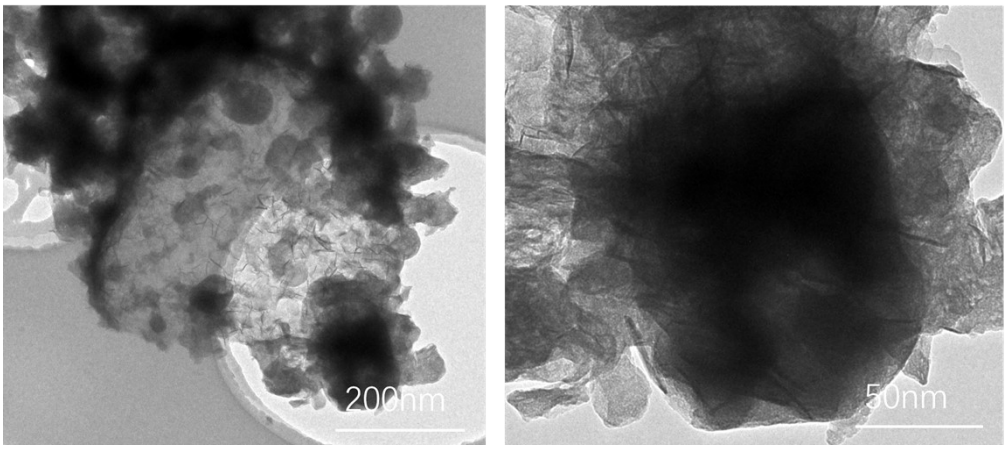

b

Figure S2. (a) SEM mapping of NCM111. (b) TEM image of NCM111.

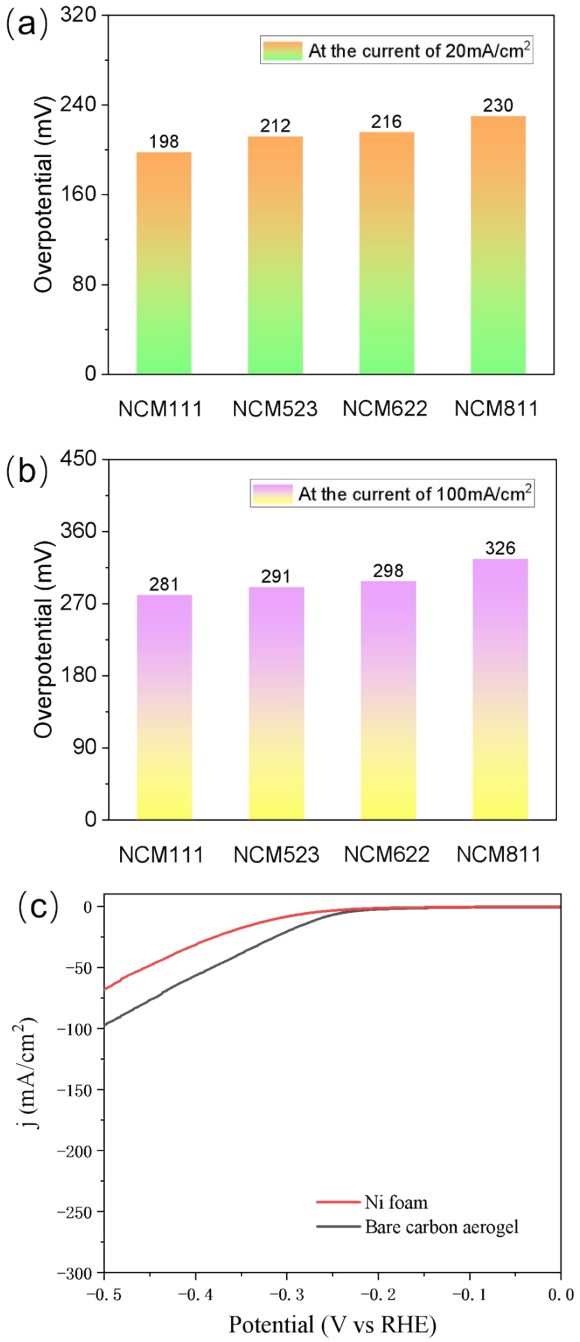

Figure S3. (a) The HER overpotential of NCM111 at the current density of 20 mA/cm^2. (b) The HER overpotential of NCM111 at the current density of 100 mA/cm^2. (c) HER polarization curves of bare carbon aerogel and Ni foam in 1.0 M KOH at a scan rate of 5 mV/s.

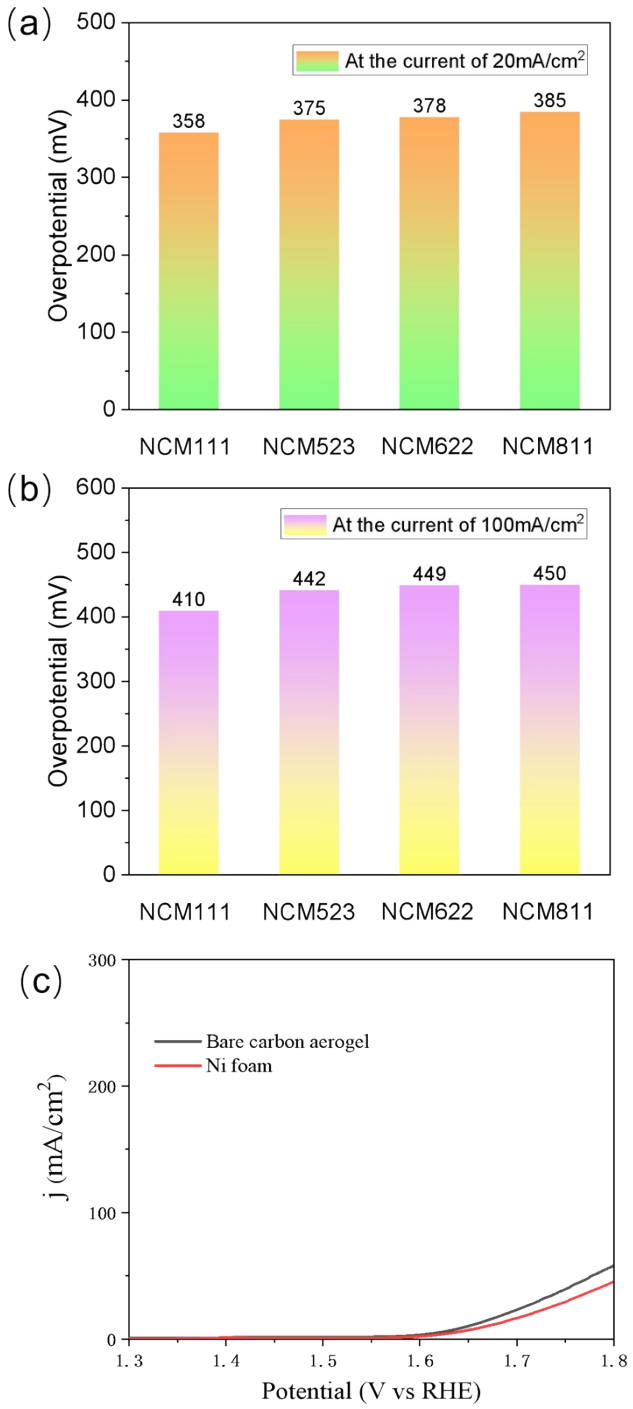

Figure S4. (a) The OER overpotential of NCM111 at the current density of 20 mA/cm^2. (b) The OER overpotential of NCM111 at the current density of 100 mA/cm^2. (c) OER polarization curves of bare carbon aerogel and Ni foam in 1.0 M KOH at a scan rate of 5 mV/s.

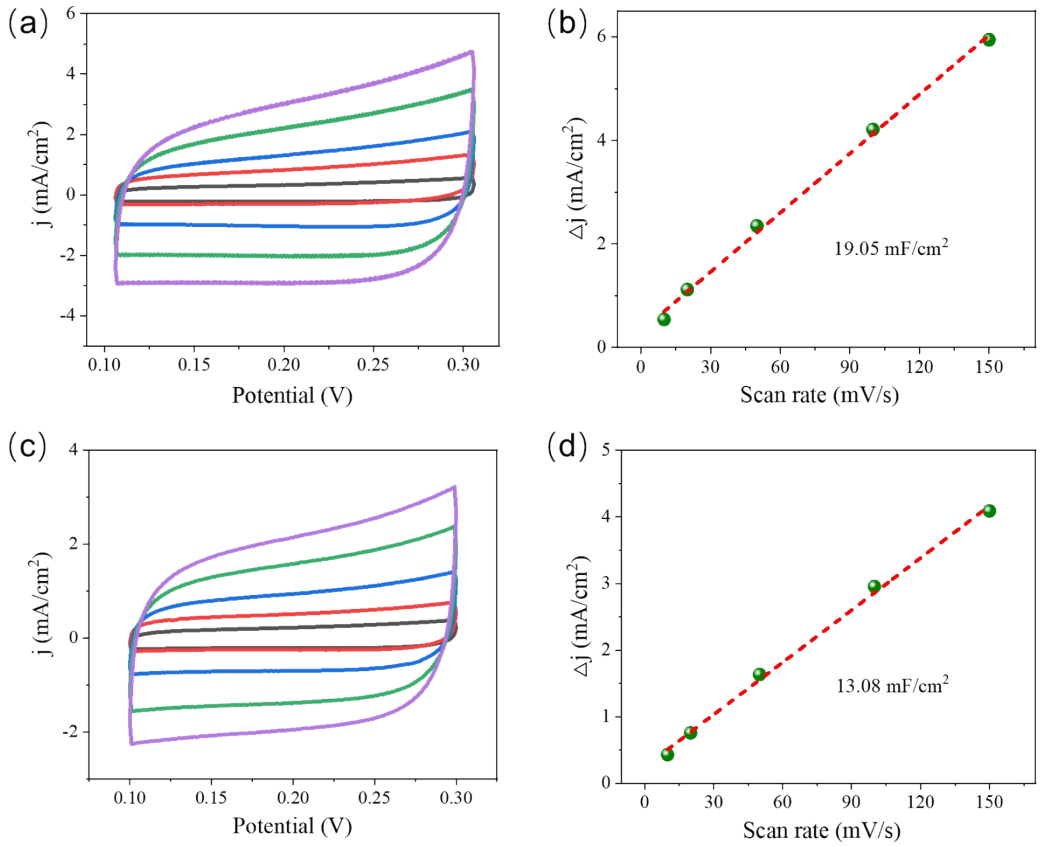

Figure S5. (a) CVs of NCM111 at potential from 0.1 V to 0.3 V vs RHE at scan rates of 20 mV/s, 50 mV/s, 80 mV/s, 110 mV/s and 140 mV/s. (b) The capacitive current densities of NCM111 measured at 0.1 V vs RHE with different scan rates. (c) CVs of NCM523 at potential from 0.1 V to 0.3 V vs RHE at scan rates of 20 mV/s, 50 mV/s, 80 mV/s, 110 mV/s and 140 mV/s. (d) The capacitive current densities of NCM523 measured at 0.1 V vs RHE with different scan rates.

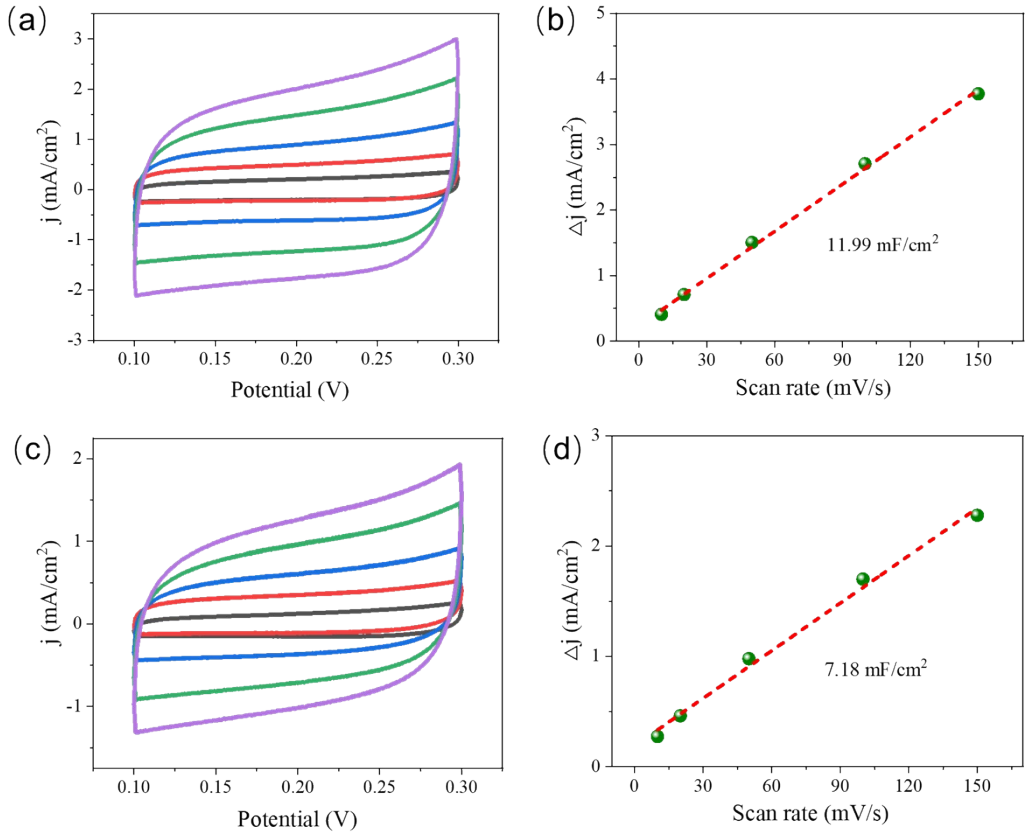

Figure S6. (a) CVs of NCM622 at potential from 0.1 V to 0.3 V vs RHE at scan rates of 20 mV/s, 50 mV/s, 80 mV/s, 110 mV/s and 140 mV/s. (b) The capacitive current densities of NCM622 measured at 0.1 V vs RHE with different scan rates. (c) CVs of NCM811 at potential from 0.1 V to 0.3 V vs RHE at scan rates of 20 mV/s, 50 mV/s, 80 mV/s, 110 mV/s and 140 mV/s. (d) The capacitive current densities of NCM811 measured at 0.1 V vs RHE with different scan rates.

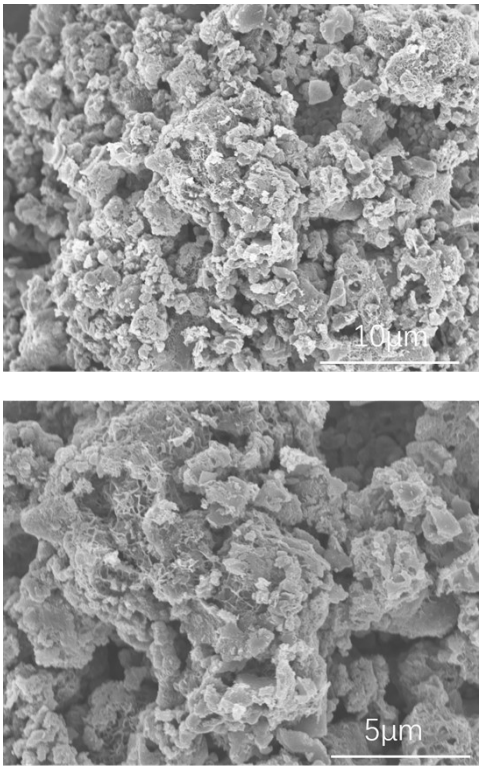

Figure S7 SEM image of NCM111 after the stability evaluation.

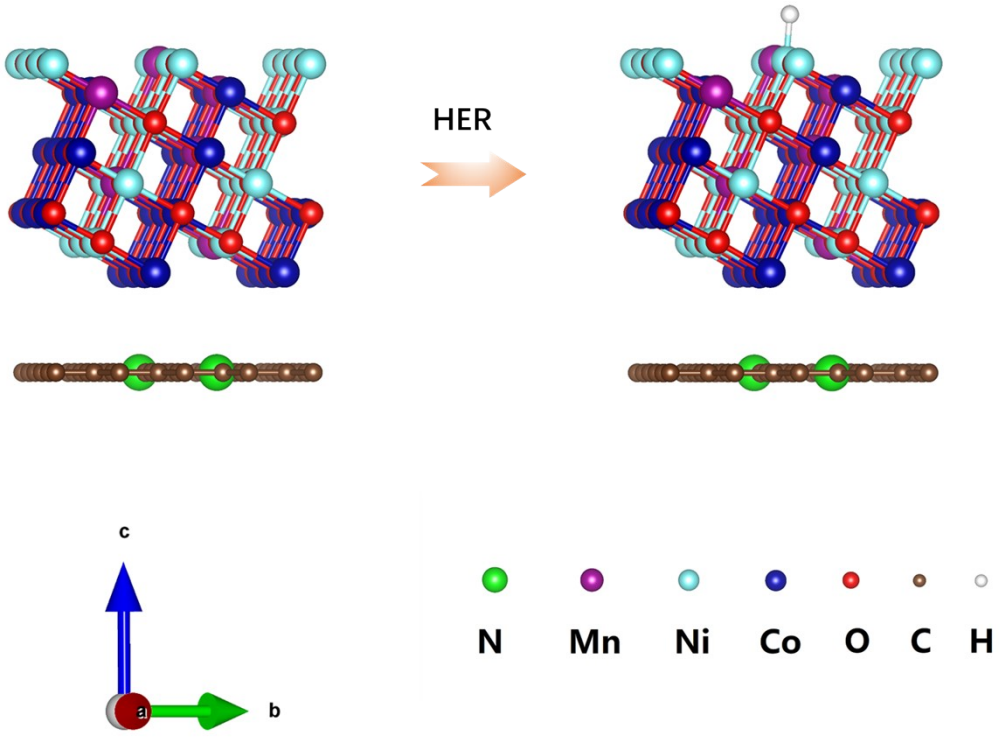

Figure S8. Schematic diagram of molecular structure of HER process.

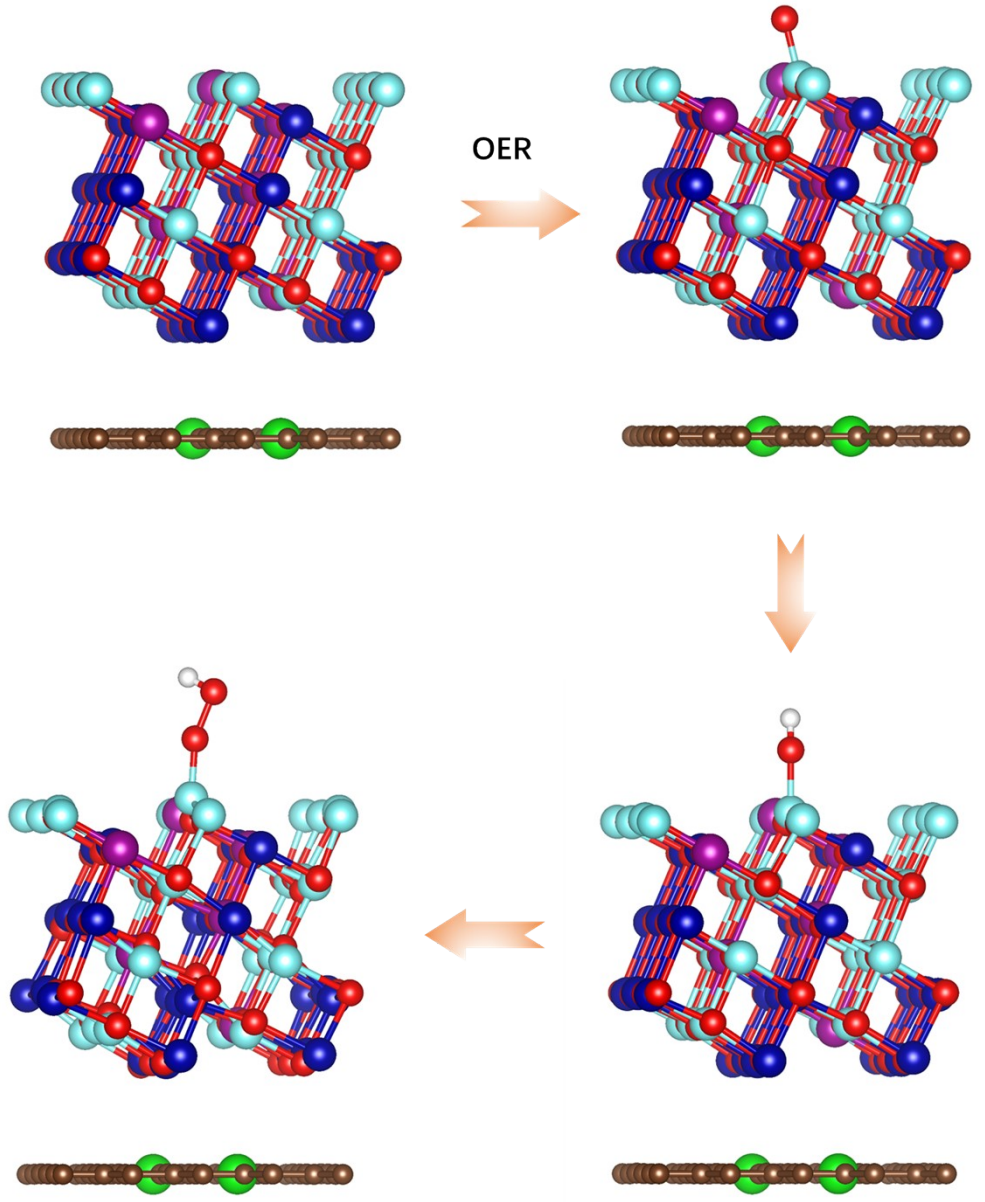

Figure S9. Schematic diagram of molecular structure of OER process.

Table S1 The state-of-the-art comparison table with previously reported catalysts

Materials	HER	OER	Ref.
CuO–ZnO	low onset potential of 1.4 V	low onset potential of 0.15 V	[1]
CoP-InNC@CNT	10 mA cm^2—159mV	10 mA cm^2—270mV	[2]
Pt/C	10 mA cm^2—37mV	/	
Ir/C	/	10 mA cm^2—295mV	
MOF with $Co_2N_2O_8$ SBUs	10 mA cm^2—196mV	10 mA cm^2—180mV	[3]
Co/Ni-doped MAF-4/ZIF-8	10 mA cm^2—183mV	10 mA cm^2—313mV	[4]
RuO_2	/	10 mA cm^2—376mV	
IrO_2	/	10 mA cm^2—406mV	
Zn-doped RuO_2	/	10 mA cm^2—173mV	[5]
RuO_2	/	100 mA cm^2—377mV	
$TiMn_2$	10 mA cm^2—139mV	/	[6]
Pt/C	10 mA cm^2—34mV	/	
Pt@RuO_x	10 mA cm^2—20mV	10 mA cm^2—157mV	[7]
Tantalum-induced reconstruction of Ni_3S_2	10 mA cm^2—56mV	10 mA cm^2—242mV	[8]
Mo/1T-MOS_2	10 mA cm^2—151mV	/	[9]
Pt/C	10 mA cm^2—73mV	/	
Fe/W-Ni_3S_2	10 mA cm^2—222mV	10 mA cm^2—174mV	[10]
FeCoNiPtRu high-entropy alloy	10 mA cm^2—104mV	10 mA cm^2—331mV	[11]
RuP/$CoNiP_4O_{12}$//CC	10 mA cm^2—27mV	10 mA cm^2—227mV	[12]
RuO_2	/	100 mA cm^2—345mV	
Superaerophobic nickel-coated catalysts on Chinese rice paper	10 mA cm^2—87mV	20 mA cm^2—250mV	[13]
NCM	10 mA cm^2—198mV	20 mA cm^2—358mV	This work

References

[1] M.P. Kumar, N. Kumaresan, R.V. Mangalaraja, I. Zaporotskova, A. Arulraj, G. Murugadoss, A. Pugazhendhi, Zinc oxide nanoflakes supported copper oxide nanosheets as a bifunctional electrocatalyst for OER and HER in an alkaline medium, Environmental Research, 2024, 252: 119030.
[2] L. Chai, Z. Hu, X. Wang, Y. Xu, L. Zhang, T.-T. Li, Y. Hu, J. Qian, S. Huang, Stringing Bimetallic Metal-Organic Framework-Derived Cobalt Phosphide Composite for High-Efficiency Overall Water Splitting, Advanced Science, 2020, 7(5): 1903195.
[3] L. Wang, C. Fan, J. Wang, R. Wu, X. Zhang, D. Zhang, Y. Zhao, Y. Fan, Adjusting organic ligands to construct four 3D metal-organic frameworks with Co2N2O8 SBUs as efficient bifunctional electrocatalysts for OER and HER, Journal of Molecular Structure, 2024, 1315: 138993.
[4] J.-X. Wu, W.-X. Chen, C.-T. He, K. Zheng, L.-L. Zhuo, Z.-H. Zhao, J.-P. Zhang, Atomically Dispersed Dual-Metal Sites Showing Unique Reactivity and Dynamism for Electrocatalysis, Nano-Micro Letters, 2023, 15(1): 120.
[5] D. Zhang, M. Li, X. Yong, H. Song, G.I.N. Waterhouse, Y. Yi, B. Xue, D. Zhang, B. Liu, S. Lu, Construction of Zn-doped RuO2 nanowires for efficient and stable water oxidation in acidic media, Nature Communications, 2023, 14(1): 2517.
[6] R. Jain, R. Raj, M. Ram, A. Rani, S.G. Dastider, R.S. Dhayal, K.K. Haldar, TiMn2 based bimetallic nano alloy electrocatalyst for improve hydrogen evolution reaction, Discover Electrochemistry, 2024, 1(1): 1-12.
[7] Z. Peng, Q. Zhang, G. Qi, H. Zhang, Q. Liu, G. Hu, J. Luo, X. Liu, Nanostructured Pt@RuOx catalyst for boosting overall acidic seawater splitting, Chinese Journal of Structural Chemistry, 2024, 43(1): 100191.
[8] X. Liu, M. Liu, H. Liao, S. Zhang, X. He, Y. Yu, L. Li, P. Tan, F. Liu, J. Pan, Tantalum-induced reconstruction of nickel sulfide for enhanced bifunctional water splitting: Separate activation of the lattice oxygen oxidation and hydrogen spillover, Journal of Colloid and Interface Science, 2025, 680: 568-577.
[9] Z. Wang, Z. Guo, Y. Gao, D. Wang, X. Cui, Stable Mo/1T-MoS2 Monolith Catalyst with a Metallic Interface for Large Current Water Splitting, ACS Applied Materials & Interfaces, 2023, 15(11): 14206-14214.
[10] S. Wang, D. Yuan, S. Sun, S. Huang, Y. Wu, L. Zhang, S.X. Dou, H.K. Liu, Y. Dou, J. Xu, Iron, Tungsten Dual-Doped Nickel Sulfide as Efficient Bifunctional Catalyst for Overall Water Splitting, Small, 2024, 20(36): 2311770.
[11] M. Geng, Y. Zhu, J. Guan, R. Zhang, Q. Zou, L. Wang, B. Guo, M. Zhang, Carbothermal shock synthesis of FeCoNiPtRu high-entropy alloy for dual-function water splitting in alkaline media, Journal of Alloys and Compounds, 2024, 1005: 176180.
[12] J. Zhao, Y. Zhang, Y. Xia, B. Zhang, Y. Du, B. Song, H.-L. Wang, S. Li, P. Xu, Strong phosphide-metaphosphate interaction in RuP/CoNiP4O12 for enhanced electrocatalytic water splitting, Applied Catalysis B: Environmental, 2023, 328: 122447.
[13] X. Hao, Q. Sun, K. Hu, Y. He, T. Zhang, D. Zhang, X. Huang, X. Liu, Enhancing electrochemical water-splitting efficiency with superaerophobic nickel-coated catalysts on Chinese rice paper, Journal of Colloid and Interface Science, 2024, 673: 874-882.